Small-Scale Structures in Three-Dimensional Magnetohydrodynamic Turbulence

P. D. Mininni,[1] A. G. Pouquet,[1] and D. C. Montgomery[2]

[1]*National Center for Atmospheric Research, P.O. Box 3000, Boulder, Colorado 80307, USA*

[2]*Department of Physics and Astronomy, Dartmouth College, Hanover, New Hampshire 03755, USA*

(Received 28 July 2006; published 14 December 2006)

We investigate using direct numerical simulations with grids up to 1536^3 points, the rate at which small scales develop in a decaying three-dimensional MHD flow both for deterministic and random initial conditions. Parallel current and vorticity sheets form at the same spatial locations, and further destabilize and fold or roll up after an initial exponential phase. At high Reynolds numbers, a self-similar evolution of the current and vorticity maxima is found, in which they grow as a cubic power of time; the flow then reaches a finite dissipation rate independent of the Reynolds number.

DOI: 10.1103/PhysRevLett.97.244503 PACS numbers: 47.27.Jv, 47.65.−d, 95.30.Qd

Magnetic fields are ubiquitous in the cosmos and play an important dynamical role in the solar wind, in stars, or the interstellar medium. The associated flows have large but finite Reynolds numbers, and nonlinear mode coupling leads to the formation of intermittent structures; viscosity ν and magnetic diffusivity η also play a role; "tearing mode"-like behavior develops and reconnection takes place. Questions arise as to how rapidly dissipation occurs as the Reynolds numbers increase, what the origin of the intermittent structures is, and how fast they form.

For these long-standing problems, e.g., in the context of reconnection events in the magnetopause or in heating of stellar coronas, many other phenomena may play an important part, such as compressibility or ionization. These can lead to a more complex Ohm's law with, e.g., a Hall current, or to the inclusion of radiative or gravitational processes. Many aspects of the two-dimensional (2D) case are understood, but the three-dimensional (3D) case remains more obscure. Early 3D work [1] showed that the topology of a reconnecting region, more complex than in 2D, can lead to more varied behavior.

In the ideal (nondissipative, Euler) limit, a criterion for discriminating between singular and regular behavior in the absence of magnetic fields follows from the seminal work of Beale, Kato, and Majda (hereafter, BKM) [2]: for a singularity to develop, the time integral of the supremum of the vorticity must grow as $(t_* - t)^{-\alpha}$, with $\alpha > 1$ and t_* the time of formation of a singularity. In MHD [3], one deals with the Elsässer fields $\mathbf{z}^{\pm} = \mathbf{v} \pm \mathbf{b}$ with $\mathbf{v}$ the velocity, and $\mathbf{b} = \nabla \times \mathbf{A}$ the induction in dimensionless Alfvénic units ($\mathbf{A}$ is the vector potential). Intense current sheets form at either magnetic nulls ($\mathbf{b} = 0$) or when not all components of the magnetic field go to zero or otherwise develop strong gradients; in 2D, a vortex quadrupole is associated with these structures. The occurrence of MHD singularities has been sought in direct numerical simulations (DNS) with either regular [4,5] or adaptive grids [6], and with different initial configurations. No clear conclusion has emerged because of the need to resolve a large range of scales. Reference [7] (and references therein) discuss the Euler case. Both laboratory experiments and DNS have also studied the resulting acceleration of particles around the reconnection region [8].

The early development of small scales in such flows is thought to be exponential [9] because the large-scale gradients of the velocity and magnetic fields, assumed given, stretch the vorticity and current, but what happens beyond the linear stage remains unclear. In 2D, numerical simulations with periodic boundary conditions show that the late-time evolution of nondissipative MHD remains at most exponential [10]. This point was later confirmed theoretically [11] by examining the structure around hyperbolic nulls, before finite dissipation sets in [12]. In 3D, most initial conditions develop sheets that seem to render the problem quasi-two-dimensional locally. 3D MHD flows display a growth of small scales of an exponential nature, though it is possible that in the ideal case a singular behavior may emerge at later times [6].

In this Letter, we address the early development of structures in 3D in the presence of dissipation. The incompressible MHD equations read, with $\mathcal{P}$ the pressure:

$$\frac{\partial \mathbf{v}}{\partial t} + \mathbf{v} \cdot \nabla \mathbf{v} = -\frac{1}{\rho}\nabla \mathcal{P} + \mathbf{j} \times \mathbf{b} + \nu \nabla^2 \mathbf{v}, \qquad \frac{\partial \mathbf{b}}{\partial t} = \nabla \times (\mathbf{v} \times \mathbf{b}) + \eta \nabla^2 \mathbf{b}; \tag{1}$$

$\rho = 1$ is the density and $\nabla \cdot \mathbf{v} = 0$, $\nabla \cdot \mathbf{b} = 0$. With $\nu = 0$, $\eta = 0$ the energy $E = \langle v^2 + b^2 \rangle / 2$ and cross helicity $H_C = \langle \mathbf{v} \cdot \mathbf{b} \rangle / 2$, are conserved, with the magnetic helicity $H_M = \langle \mathbf{A} \cdot \mathbf{b} \rangle$ in 3D. Defining $D_{\pm}/Dt = \partial_t + \mathbf{z}^{\pm} \cdot \nabla$ with $\mathbf{z}^{\pm} = \mathbf{v} \pm \mathbf{b}$, one can symmetrize Eqs. (1):

$$\frac{D_{\mp}\mathbf{z}^{\pm}}{Dt} = -\nabla \mathcal{P} + (\nu + \eta) 2 \nabla^2 \mathbf{z}^{\pm} + (\nu - \eta) 2 \nabla^2 \mathbf{z}^{\mp}. \tag{2}$$

To study the development of structures in MHD flows, we solve Eqs. (1) numerically in a 3D box using periodic boundary conditions and a pseudospectral method, dealiazed by the standard 2/3 rule; $k_m = 1$ for a box of length $L_0 = 2\pi$, and N regularly spaced grid points lead to a

maximum wave number $k_M = N/3$. At all times, we preserve $k_D/k_M < 1$, where k_D is the dissipation wave number estimated on the Kolmogorov spectrum (at early times, the resolution requirement is less stringent).

Table I summarizes the conditions for all runs reported. It is important to emphasize that two distinct classes of initial conditions have been used, and these lead to distinct evolutions. In the first class (OT runs), we use a 3D generalization of the so-called Orszag-Tang vortex [13], which has become a prototype flow for the study of MHD turbulence, including the compressible case [14]. In the second class of runs, labeled RND, we start with a set having much less initial symmetry; these will be described in more detail below.

The 3D initial conditions for the OT runs are

$$\mathbf{v}_0 = [-2\sin y, 2\sin x, 0],$$

$$\mathbf{b}_0 = \beta[-2\sin 2y + \sin z, 2\sin x + \sin z, \sin x + \sin y].$$

The OT flow in 2D has a stagnation point in the (x, y) plane and a hyperbolic X point for the magnetic field; a 3D magnetic component is added in the z direction, resulting in a flow that has nulls of different types [15] corresponding to the signs of the eigenvalues of the $\partial_i b_j$ matrix [5]; with $\beta = 0.8$, the kinetic and magnetic energies E_V, E_M are initially equal to 2, the normalized correlation $\tilde{\rho}^c = 2\langle \mathbf{v}\cdot\mathbf{b}\rangle/(\langle v^2 + b^2\rangle)$ is $\sim$0.41, and $H_M = 0$.

We monitor the small-scale development by following the dynamical evolution of the extrema of the generalized vorticities $\nabla \times \mathbf{z}^{\pm}$ or of their individual components [16] in the spirit of the BKM criterion. Four OT runs were done with Reynolds numbers $R_e = UL/\nu$ ranging from 570 to 5600 at the time of maximum energy dissipation $\epsilon = -\nu\langle\omega^2\rangle - \eta\langle j^2\rangle$; here, $L = 2\pi \int E_V(k)k^{-1}dk/\int E_V(k)dk$ is the integral scale, $U = \langle v^2\rangle^{1/2}$ is the rms velocity, and $E_V(k)$ is the kinetic energy spectrum. Figure 1(a) shows the temporal evolution of the maximum of the current density, $\max\{j\}$, whose location can be easily identified visually; vorticity behaves in a similar fashion. After an exponential growth up to $t \sim 0.6$, corresponding to the development of linearized instabilities on the OT vortex and independent of the value of R_e, a faster self-similar growth develops $\sim t^3$, verified at high resolution.

The first temporal maximum of $\max\{j\}$ is reached at slightly later times as R_e increases; similarly [see Fig. 1(b)], the total energy dissipation ϵ shows a delay in the onset of the development of small scales as R_e grows, reminiscent of 2D behavior [12], with a slower global growth rate after the initial exponential phase; this delay, however, does not preclude reaching a quasiconstant maximum of ϵ in time as R_e grows. Whereas in the 2D case, it only obtains at later times when reconnection sets in with a multiplicity of current sheets, in the 3D case more instabilities of current and vorticity can occur and the flow becomes complex in the nonlinear phase. The dependence on R_e of the time at which the first maximum of $\max\{j\}$ is reached is slow ($\sim R_e^{0.08}$), and similarly for the time the maximum of ϵ is reached. Computations at higher R_e should be performed to confirm these results.

The sharp transition around $t = 0.6$ can be interpreted in terms of the nonlocality of interactions in MHD turbulence [17] with transfer of energy involving widely separated scales. Thus, as the flow exits the linear phase, all scales can interact simultaneously; this may be a reason why, in a computation using OT and adaptive mesh refinement [6], it was found to be difficult to go beyond $t = 0.6$ since small scales were developing abruptly in many places in the flow through prevailing nonlinearities. The energy spectra in this early phase are steep, with a power law $\sim k^{-3}$ (not

TABLE I. Runs with an Orszag-Tang vortex (OT1-4), or with large-scale ABC flows and small-scale random noise with a k^{-3} spectrum (RND1-5); N is the linear resolution.

Run	N^3	$\nu = \eta$
OT1–OT4	64^3–512^3	1×10^{-2}–7.5×10^{-4}
RND1–RND5	64^3–1536^3	8×10^{-3}–2×10^{-4}

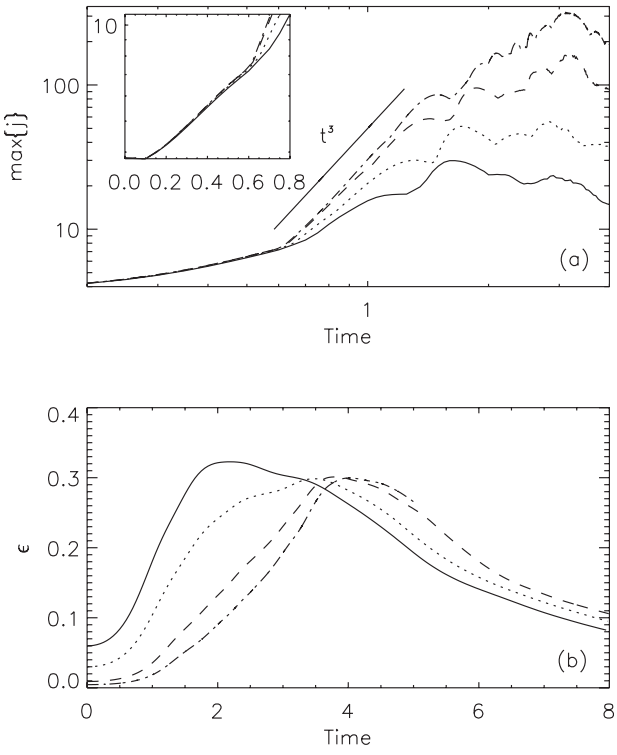

FIG. 1. (a) Evolution of the supremum of current for the OT runs in log-log. The inset shows the evolution at early times in lin-log units; a slope of t^3 is also indicated. The exponential phase ends at $t \sim 0.6$. (b) Total dissipation as a function of time for the same runs in lin-lin. $R_e = 570$ (solid line), $R_e = 1040$ (dotted line), $R_e = 3040$ (dashed line), and $R_e = 5600$ (dash-dotted line).

shown). A shallower $\sim k^{-1.70}$ spectrum develops at later times, as found in earlier works.

In view of the similarities observed between the behavior of the 3D OT vortex and its 2D counterpart, it is worth asking whether such a development may not be due to the high degree of initial symmetry in the flow. Therefore, we now consider a random initial flow constructed from Beltrami (helical) flows to which smaller-scale random fluctuations are added. The modes with $k = 1$, 2, and 3 are loaded with three ABC flows [18], while for $k > 3$, the spectrum is loaded with Gaussian random noise with an amplitude proportional to $k^{-3}\exp[-2(k/k_0)]^2$, and the phases of the modes with $k > 3$ are chosen from a Gaussian random number generator. Initially, $E_V = E_M = 0.5$, $\tilde{\rho}^c$ is $\sim 10^{-4}$, and $H_M \sim 0.45$; five runs are performed (see Table I); run RND5 on a grid of 1536^3 points is stopped when saturation of the growth of the maximum current occurs. Unlike the OT runs, there are no 2D null points or exact zeros of the magnetic field; what results is a more complex evolution than in the OT runs, but nevertheless bearing with them some striking similarities.

As seen in Fig. 2(a), both the exponential and approximately self-similar phases are noisier, as can be expected with several structures competing for the development of small-scale maxima. The two runs with highest resolution (RND4 and RND5) show a steep development consistent with a t^3 law. At lower R_e, however, a self-similar regime or something like it seems to occur at a slower pace, with growth consistent with t^2 behavior, as found in 2D at comparable resolutions. We are uncertain whether the same structure accounts for $\max\{j\}$ in this regime for all time, but its unique identification can be done in the self-similar regime.

Figure 2(b) shows the evolution of the magnetic energy spectrum at early times, during the self-similar growth phase [the evolution of $E_V(k)$ is similar]. Before $t \sim 0.6$, the largest Fourier amplitudes are of the order of the truncation error. For $t > 0.6$ all scales are nonlinearly excited and an approximately self-similar growth sets in; the energy spectra are compatible with a k^{-3} law. After the saturation of $\max\{j\}$, the slope of $E_M(k)$ increases slowly towards a $k^{-1.70}$ law. The same behavior is in fact observed in the OT run, in which no k^{-3} power law has been imposed on the initial conditions.

The structures that develop appear to be accumulations of current sheets (and similarly for the vorticity, not shown) as was found in Ref. [4]. Figure 3 shows a zoom on two such structures, with magnetic field lines indicated as well. It appears that the magnetic field does not have a local zero and only undergoes a shear as the current sheet is crossed. Loosely speaking, only one component of the magnetic field can be said to reverse sign, reminiscent of magnetospheric observations [15]. Kelvin-Helmoltz instabilities with rolling up of such sheets are also present in this turbulent flow but only at the highest Reynolds number

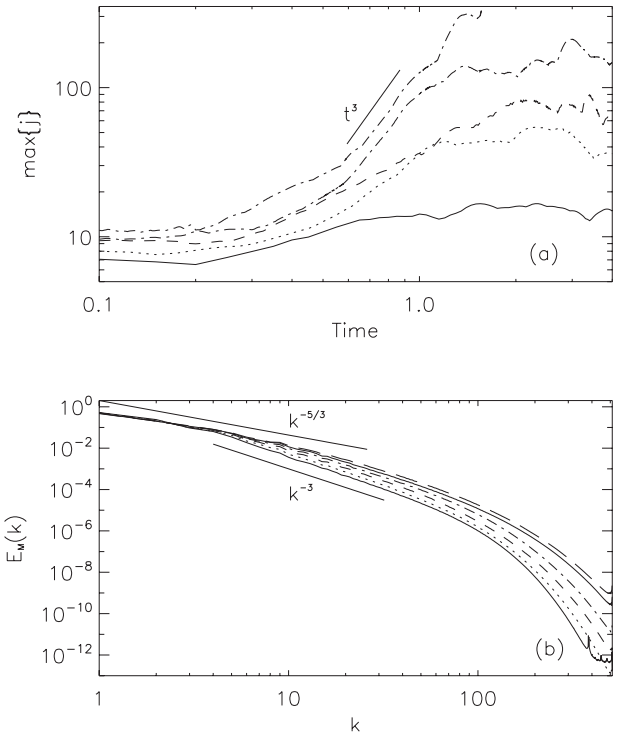

FIG. 2. (a) Evolution of the supremum of the current density in log-log for runs RND1 to RND5, with $R_e = 690$ (solid line), $R_e = 1300$ (dotted line), $R_e = 2300$ (dashed line), $R_e = 4200$ (dot-dashed line), and $R_e = 10\,100$ (long dashed line). At high R_e, a power law consistent with t^3 is recovered. (b) Magnetic energy spectra at early times in run RND5. The lines (from below) correspond to $t = 0.6$ up to $t = 1.6$ with temporal increments of 0.2. Slopes of k^{-3} and $k^{-5/3}$ are indicated as a reference.

(run RND5); at lower R_e the sheets are thicker, the instability is too slow, and only folding of such sheets occurs. Magnetic field lines are parallel to the roll in such a way that magnetic tension does not prevent the occurrence of the instability. Note that folding of magnetic structures has been advocated in the context of MHD at large magnetic Prandtl number [19]. Alfvenization of the flow ($\mathbf{v} = \pm\mathbf{b}$) is rather strong in the vicinity of the sheets, with $0.7 \leq |\tilde{\rho}^c| \leq 1$, although globally the flow remains uncorrelated ($\tilde{\rho}^c \sim 4 \times 10^{-4}$); this local Alfvénization gives stability to such structures since the nonlinear terms are weakened, in much the same way vortex tubes in Navier-Stokes flows are long-lived because of (partial) Beltramization ($\mathbf{v} \sim \pm\boldsymbol{\omega}$). Moreover, within the sheet $\tilde{\rho}^c > 0$, and it is negative outside, with a slight predominance of $\mathbf{b}$. All of this indicates that a double velocity-magnetic field shear plays an important role in the development of small scales in MHD.

There is an elementary, analytically soluble, one-dimensional model that illustrates sharply the role that velocity shear can play in enhancing current intensity, e.g., during early dynamo activity [20]. This consists of two semi-infinite slabs of rigid metal with equal conduc-

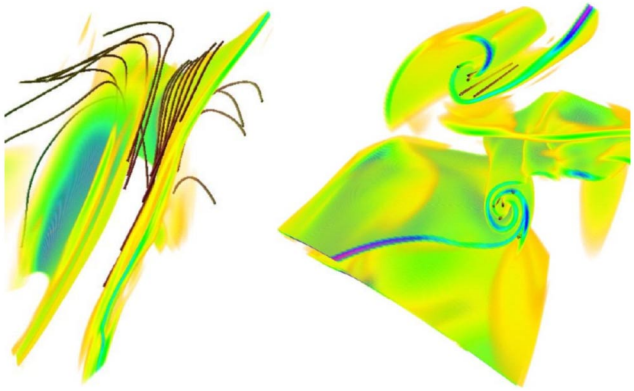

FIG. 3 (color online). Regions of strong current density, and magnetic field lines in their vicinity for run RND5 at $t = 1.6$. The region at left has $450^2 \times 250$ points, and that at right has $260 \times 160 \times 200$. The sheets are thin and elongated (up to $1/3$ the size of the box); the magnetic field lines are parallel to the sheet and quasiorthogonal to each other on each side of it, and they depart from the sheet transversally. Both folding (left) and rolling (right) occurs at this R_e. Vortex sheets (not shown) are colocated and parallel to the current sheets.

tivities, at rest against each other at the plane $y = 0$, say. A uniform dc magnetic field $\mathbf{b}_0$ is perpendicular to the interface and penetrates both slabs. At time $t = 0$, the slabs are impulsively forced to slide past each other in the x direction with equal and opposite velocities ($\mathbf{v}_0$, say). The developing (quasimagnetostatic) field, which acquires an x component, is a function of y and t only, and is governed by diffusion equations above and below the plane $y = 0$. Matching tangential components of the electric field immediately above and below the interface reduces the pair to a soluble diffusion equation with a jump in the y derivative at $y = 0$. The resulting magnetic field is expressible in terms of complementary error functions and grows without bound, as does the total Ohmic dissipation. The introduction of a time dependence in $\mathbf{v}_0$ may allow also for solutions in which the maximum of the current grows as a power law in time.

In conclusion, high resolution simulations of the early stages in the development of MHD turbulence allowed us to study the creation and evolution of small-scale structures in three-dimensional flows. We are still unable to determine conclusively whether or not singularities will occur in such flows, but at the present Reynolds numbers, the BKM criterion is not fulfilled and higher-resolution runs are needed. Roll-up of current and vortex sheets, and a self-similar growth of current and vorticity maxima, was found, features that to the best of our knowledge were not reported in previous simulations at smaller Reynolds numbers. Also, a convergence of the maximum dissipation rate to a value independent of R_e was found. More analysis will be carried out to understand how structures are formed, the relevance of the development of alignment between the velocity and magnetic fields and its connection to universal behavior in MHD flows [21], and the creation and role of local exact solutions to the MHD equations, such as Alfvén waves.

NSF Grants No. CMG-0327888 and ATM-0327533 are acknowledged. Computer time was provided by NCAR and 3D visualizations were done using VAPoR [22].

[1] J. M. Greene, Journal of Geophysical Research (Space Physics) **93(A8)**, 8583 (1988).
[2] J. Beale, T. Kato, and A. Majda, Commun. Math. Phys. **94**, 61 (1984).
[3] R. Calflisch, I. Klapper, and G. Steele, Commun. Math. Phys. **184**, 443 (1997).
[4] H. Politano, A. Pouquet, and P. L. Sulem, Phys. Plasmas **2**, 2931 (1995).
[5] R. Kerr and A. Brandenburg, Phys. Rev. Lett. **83**, 1155 (1999); see also physics/0001016.
[6] R. Grauer and C. Marliani, Phys. Rev. Lett. **84**, 4850 (2000).
[7] R. Kerr, Phys. Fluids A **17**, 075103 (2005).
[8] N. Wild, W. Gekelman, and R. Stenzel, Phys. Rev. Lett. **46**, 339 (1981); Y. Ono *et al.*, Phys. Rev. Lett. **76**, 3328 (1996); D. Knoll and J. Brackbill, Phys. Plasmas **9**, 3775 (2002); M. R. Brown *et al.*, Phys. Plasmas **9**, 2077 (2002).
[9] I. Syrovatskii, Sov. Phys. JETP **33**, 933 (1971).
[10] U. Frisch *et al.*, J. Mec. Theor. Appl. **2**, 191 (1983).
[11] I. Klapper, A. Rado, and M. Tabor, Phys. Plasmas **3**, 4281 (1996).
[12] D. Biskamp and H. Welter, Phys. Fluids B **1**, 1964 (1989); H. Politano, A. Pouquet, and P. L. Sulem, Phys. Fluids B **1**, 2330 (1989).
[13] S. Orszag and C. Tang, J. Fluid Mech. **90**, 129 (1979).
[14] J. Picone and R. Dahlburg, Phys. Fluids B **3**, 29 (1991).
[15] K. Nykyri *et al.*, Ann. Geophys. **24**, 1 (2006).
[16] One may also monitor the symmetrized gradient matrices, as well as the total entrophy production [5].
[17] A. Alexakis, P. D. Mininni, and A. Pouquet, Phys. Rev. E **72**, 046301 (2005); P. D. Mininni, A. Alexakis, and A. Pouquet, Phys. Rev. E **72**, 046302 (2005).
[18] V. I. Arnol'd, C. R. Acad. Sci. Paris Ser. IV **261**, 17 (1965); D. Galloway and U. Frisch, Geophys. Astrophys. Fluid Dyn. **36**, 58 (1986).
[19] A. Schekochihin *et al.*, Astrophys. J. **576**, 806 (2002).
[20] D. C. Montgomery, P. D. Mininni, and A. Pouquet, Bull. Am. Phys. Soc., Ser. II **50**, 177 (2005).
[21] A. Pouquet *et al.*, "Small-Scale Structures in Magneto-hydrodynamic Turbulence," edited by Y. Kaneda, IUTAM Conference (Springer-Verlag, Berlin, to be published).
[22] J. Clyne and M. Rast, in *Visualization and Data Analysis 2005*, edited by R. F. Erbacher *et al.* (SPIE, Bellingham, WA 2005), p. 284; http://www.vapor.ucar.edu.